Int. J. Solids Structures Vol. 30, No. 23, pp. 3233–3244, 1993
Printed in Great Britain

0020–7683/93 $6.00+ .00

MIXED-MODE QUANTIFICATION FOR DYNAMIC FRACTURE INITIATION: APPLICATION TO THE COMPACT COMPRESSION SPECIMEN

H. MAIGRE and D. RITTEL
Laboratoire de Mécanique des Solides, U.R.A. 317-C.N.R.S., Ecole Polytechnique, F-91128 Palaiseau Cedex, France

(*Received* 7 *December* 1992; *in revised form* 5 *June* 1993)

Abstract—This paper addresses the problem of mode-mixity for dynamic crack initiation experiments. We develop further our previously introduced approach based on the dynamic path independent H-integral and its experimental implementation on the Compact Compression Specimen (CCS) (Bui *et al.*, 1992, *Int. J. Solids Structures*, **29**(23), 2881–2895). Specifically, a procedure for mixed-mode separation into symmetric and anti-symmetric components of the H-integral is presented and verified numerically. Each component is shown to verify path-independence. The corresponding stress intensity factors are calculated and it is noted that, regardless of the crack length, mode I is the predominant crack opening mode past a short period of quantified mode-mixity. The procedure for mode-separation is applied to two experiments carried out on steel and PMMA (one specimen of each material). In these experiments, it is shown that crack initiation occurred effectively under dominant mode I. Consequently, the complete evolution of the mode I and II stress intensity factors can easily be determined in experimental testing of CCS. Correspondingly, provided we have accurate determination of the time to fracture, the crack initiation mode can be characterized.

1. INTRODUCTION

Mixed-mode crack initiation and propagation occurs frequently in dynamic fracture experiments even when it is not planned initially. This is related to wave propagation effects and to the symmetry of the specimen and applied loads. By contrast, the crack opening mode is much better controlled in static fracture experiments (generation of pure mode I or II). The extent of a likely mixed-mode must thus be assessed by quantifying each transient stress intensity factor as a necessary step toward improved experimental procedures.

Mode-mixity has been studied analytically by Lee and Freund (1990) for an infinite plate with an edge crack. Although the transient loading was chosen such as to generate essentially mode II, this study shows the development of a significant mode I component. The Coherent Gradient Sensor method (Tippur *et al.*, 1991) was applied by Mason *et al.* (1992) to study the above-mentioned problem and good agreement was found between experimental and theoretical results. An experimental study of Izod-like specimens was carried out by Kalthoff and Podleschny (1992). Mode-mixity was quantified as a function of time and the applicability of this fracture test to different materials was discussed. Nakano *et al.* (1992) used a precracked disk loaded in a one-point impact apparatus. The inclination of the center crack with respect to the line of loading determines the degree of mode-mixity.

Elastodynamic path-independent integrals have been investigated by several authors [see e.g. Nilsson (1973), Freund and Rice (1974), Gurtin (1976), Bui and Maigre (1988) and Freund (1990)]. Bui *et al.* (1992) used the H-integral to calculate dynamic stress intensity factors and applied this approach to the Compact Compression Specimen (CCS). An example of mode I dynamic fracture toughness determination was given by Rittel *et al.* (1992) for a steel CCS with a blunt notch.

However, even though the problem of mode-mixity was mentioned in both papers, it was not studied *per se*. Consequently, this paper addresses the issue of mode-mixity and quantification of the I and II components generated during the experimental testing of Compact Compression Specimens. First, we briefly recall some theoretical and experimental aspects related to the H-integral and CCS (Section 2). Next, we describe our procedure for mode separation and show numerical results on the path independence of the H-integral

(Section 3). Finally, we present experimental results about dynamic crack initiation in steel and PMMA specimens (Section 4).

2. THE H-INTEGRAL AND THE COMPACT COMPRESSION SPECIMEN

$H(\tau)$ is a path-independent integral which combines experimental and reference displacement fields (respectively **u** and **v**) and associated quantities through time convolution products (Bui and Maigre, 1988; Bui *et al.*, 1992). This concept applies to two-dimensional, linear elastic solids. Two different specific paths can be chosen for the evaluation of H: the first along the external boundary of the structure, and the second in the vicinity of the crack-tip.

The expression for $H(\tau)$ evaluated along the boundary S of a structure containing a crack of length a with applied surface tractions **T[u]** is given by:

$$H(\tau) := \frac{1}{2}\int_S \left\{ \mathbf{T}[\mathbf{u}] * \frac{\partial \mathbf{v}}{\partial a} - \frac{\partial \mathbf{T}[\mathbf{v}]}{\partial a} * \mathbf{u} \right\} \mathrm{d}S \tag{1a}$$

(* denotes time convolution product).

In the vicinity of the crack-tip, the general expression of $H(\tau)$ under plane strain conditions involves the mode I and mode II stress intensity factors for arbitrary loading:

$$H(\tau) := \frac{1-\nu^2}{E}\left(K^{\mathbf{u}}_{\mathrm{Id}} * K^{\mathbf{v}}_{\mathrm{Id}} + K^{\mathbf{u}}_{\mathrm{IId}} * K^{\mathbf{v}}_{\mathrm{IId}}\right) \tag{1b}$$

(E and ν are Young's modulus and Poisson's ratio respectively).

Therefore, due to the path-independence of H, local quantities (stress intensity factors) that are usually difficult to measure experimentally can be assessed from global information collected on the boundary of the structure. In pure I or II mode, the dynamic stress intensity factor is determined by solving a linear convolution equation of the type:

$$K^{\mathbf{v}}_{i\mathrm{d}} * K^{\mathbf{u}}_{i\mathrm{d}} = H(\tau; \mathbf{u}, \mathbf{v}) \quad i = \mathrm{I}, \mathrm{II}. \tag{2}$$

Both **v** and $K^{\mathbf{v}}_{i\mathrm{d}}$ are reference data which are determined once and for all for a given set of experiments. This approach was implemented and validated experimentally using a split Hopkinson (Kolsky) bar to apply and measure dynamic loads on the interfaces between the compact Compression Specimen and the bars (Bui *et al.*, 1992). This specimen is inserted directly between the bars and does not require additional fixtures (Fig. 1): crack opening upon application of compressive loads results from the specimen's geometry only. The CCS has a symmetric geometry but loading is not symmetric. Therefore, mode-mixity is likely to develop and must be characterized. With the terminology of *reference* and *experimental* for the various quantities, (1) now becomes:

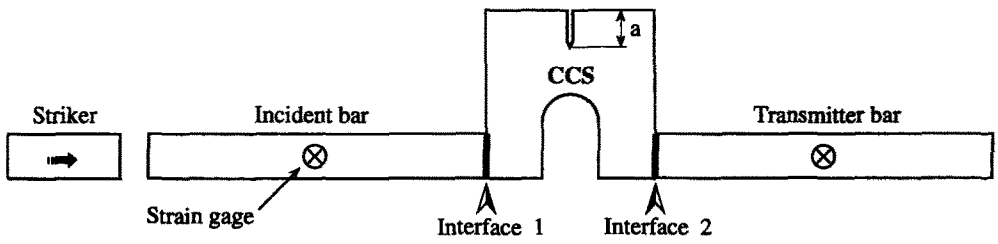

Fig. 1. Compact Compression Specimen inserted in the split Hopkinson (Kolsky) bar apparatus. Forces and displacements are applied and measured on the interfaces.

$$H(\tau) = F_{\exp} * \frac{\partial \bar{u}_{\text{ref}}}{\partial a} = \frac{1-\nu^2}{E}(K_{\text{Id}}^{\text{uexp}} * K_{\text{Id}}^{\text{uref}} + K_{\text{IId}}^{\text{uexp}} * K_{\text{IId}}^{\text{uref}}), \tag{3}$$

where $F_{\exp}$ denotes the applied force and $\bar{u}_{\text{ref}}$ the average displacement at the CCS–bar interface. This equation is used to separate and quantify the components of the mixed mode, as shown next.

3. MIXED-MODE SEPARATION: THEORY AND NUMERICAL RESULTS

The procedure for mixed-mode separation follows the guidelines presented by Bui (1983). Equation (3) can be split into pure mode I (4a) and pure mode II components (4b), using the superposition principle:

$$H_{\text{I}}(\tau) = F_{\text{Iexp}} * \frac{\partial \bar{u}_{\text{Iref}}}{\partial a} = \frac{1-\nu^2}{E} K_{\text{Id}}^{\text{uexp}} * K_{\text{Id}}^{\text{uref}}, \tag{4a}$$

$$H_{\text{II}}(\tau) = F_{\text{IIexp}} * \frac{\partial \bar{u}_{\text{IIref}}}{\partial a} = \frac{1-\nu^2}{E} K_{\text{IId}}^{\text{uexp}} * K_{\text{IId}}^{\text{uref}}. \tag{4b}$$

Extracting either of the experimental stress intensity factors necessitates the generation of a set of references $(\partial \bar{u}_{\text{iref}}/\partial a)$ and $K_{\text{id}}^{\text{uref}}$, $i = \text{I, II}$. The consistency of such a set can be assessed by checking for path independence of the H-integral. In the sequel, we present numerical results concerning the CCS but this approach applies to any other two-dimensional symmetric cracked structure.

Half a CCS was discretized into triangular and quadrilateral finite elements [total of 3965 nodes—6825 elements, Fig. 2(a)]. The numerical procedure, codes and applied load were identical to those reported by Bui *et al.* (1992). Boundary conditions shown in Fig. 2(b) were applied to enforce the selected mode. Crack opening displacements (COD) as a function of time were determined from the displacements of reference points located at 5.0×10^{-4} m from the crack tip, and the stress intensity factors were determined accordingly (Irwin, 1957). The selected material was commercial PMMA for which the mechanical constants listed in Table 1 were measured in our laboratory. Because of the viscosity of PMMA, we used a transfer modulus rather than Young's modulus (Wada, 1992). The former was assessed from the longitudinal wave velocity in this material (Zhao, 1992), with the assumption that at high deformation rates, the material exhibits a quasi-elastic response. The increment of virtual crack extension was set to $da = 5.0 \times 10^4$ m $(da/w = 7.14 \times 10^{-3})$. Figure 3 represents typical variations of H with time for each mode, as calculated for a specimen with a crack to ligament length ratio of $a/w = 0.44$. For each mode, H was calculated in the following way:

—once from boundary displacements [eqn (4) left-hand side], applying the same force to two slightly different crack lengths to obtain $(\partial \bar{u}_{\text{iref}}/\partial a)$.
—once from the corresponding stress intensity factors [eqn (4) right-hand side].

Here, experimental and reference stress intensity factors were purely numerical, corresponding to $K_i(a)$ and $K_i(a+da)$ respectively, $i = \text{I, II}$. Moreover, the reference force was the same for mode I and mode II calculations [$F_{\text{Iexp}} = F_{\text{IIexp}}$ in eqn (4)]. From Fig. 3, an excellent agreement is noted between boundary and near-tip values. For pure mode I, this was expected (and verified although not reported) from previous results showing a close fit between the numerical simulation and the experiment. However, mode II is more difficult to study numerically since it is the minor crack opening mode. The problem of mode II characterization was overcome by using a refined mesh [shown in Fig. 2(a)] compared to the coarser mesh used in pure mode I studies. The present results show that the path-independence of the H-integral is verified in the numerical model used for the generation of reference data.

(a)

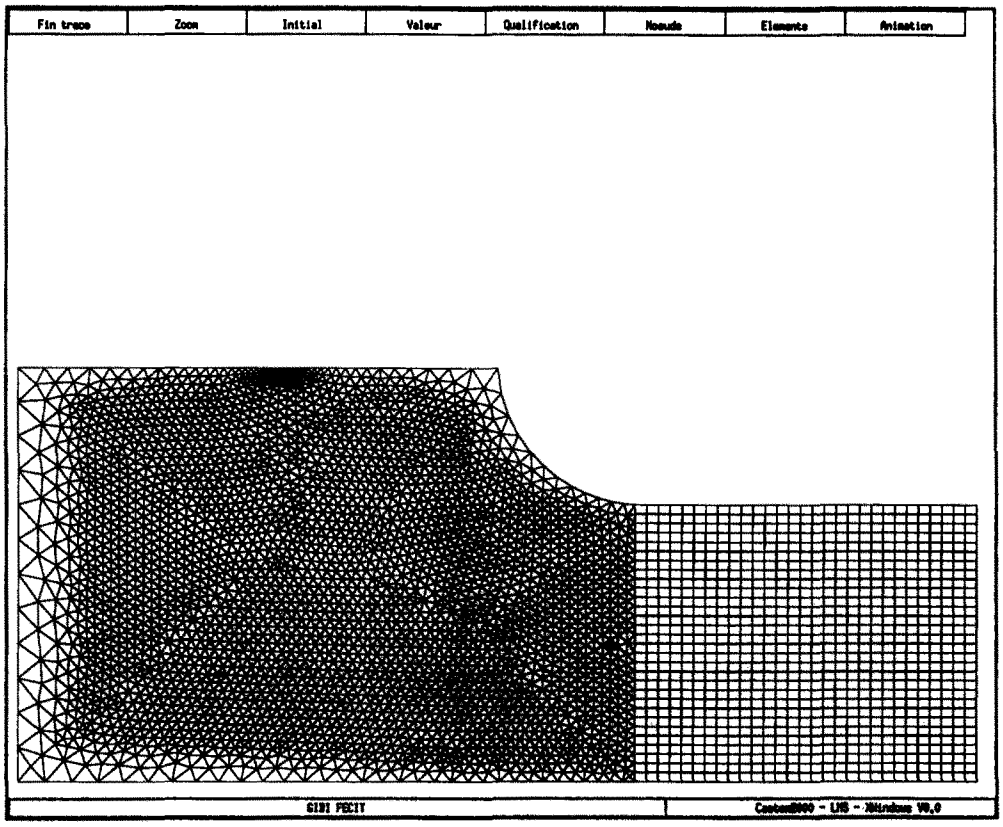

REFERENCE SPECIMEN

(b)

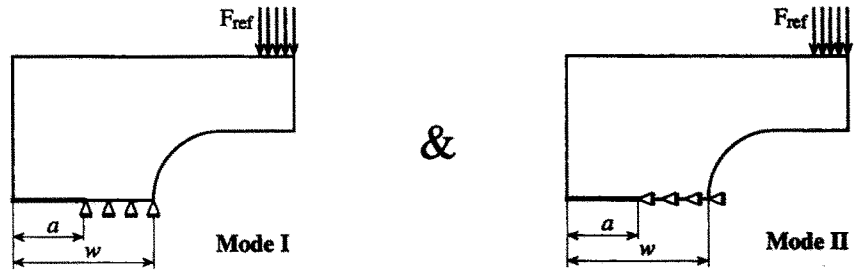

Fig. 2. (a) Discretized half-specimen for F.E. calculations. (b) Boundary conditions for pure I and II modes.

Stress intensity factors were calculated from COD values for two different ratios, $a/w = 0.44$ and $a/w = 0.63$ (Fig. 4). In both cases, it was observed that a definite mode II component develops along with the predominant mode I. Yet, the mode II contribution is much smaller than that of mode I except for very short times. Crack initiation under dominant mode I is further supported by the fact that the expression for the energy release rate involves the squared value of each stress intensity factor (Freund, 1990).

Table 1. Mechanical constants of PMMA

Transfer modulus (GPa)	Poisson's ratio	Density (kg m^{-3})
5.76	0.42	1180

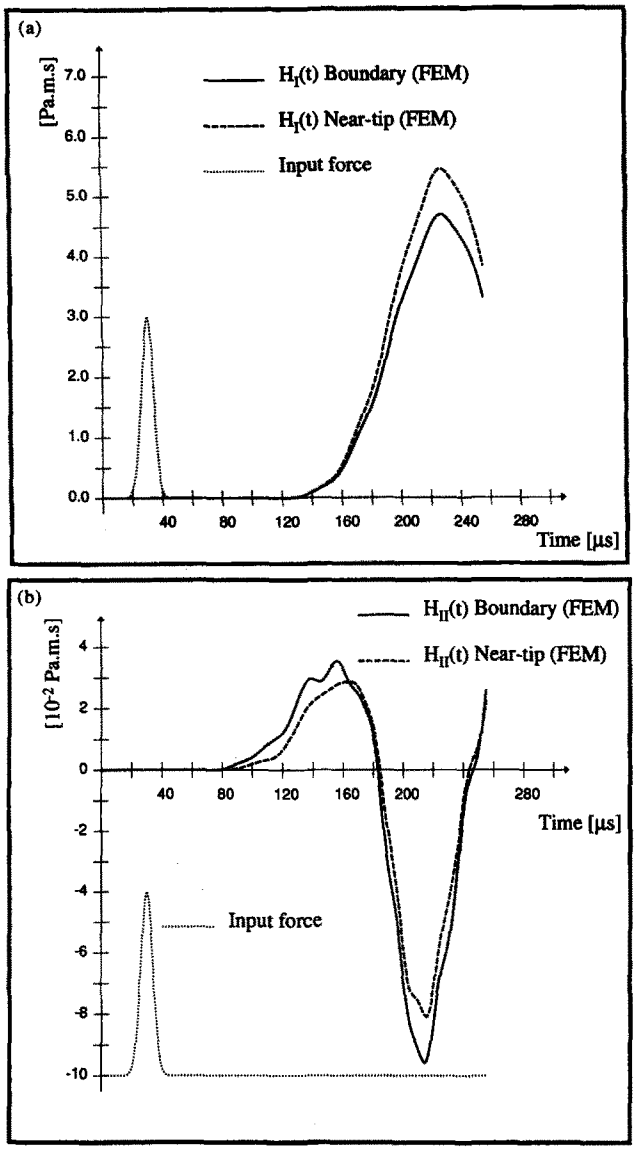

Fig. 3. PMMA reference specimen ($a/w = 0.44$): (a) H_{I} and (b) H_{II} components calculated from boundary and from local (crack-tip) data. The applied force is shown in dimensionless form.

It should also be noted that the ratio of mode I to mode II components is relatively insensitive to the a/w ratio. This is illustrated in the plot of the mixity parameter (Fig. 5) defined as $\mathcal{M}^{\mathrm{e}} = 2/\pi \tan^{-1}(K_{\mathrm{Id}}/K_{\mathrm{IId}})$ (Shih, 1974). Here, the complex (compact) specimen geometry and wave propagation pattern preclude a straightforward time normalization (e.g. by using the longitudinal wave velocity) to establish a comparison with the results of Kalthoff and Podleschny (1992).

4. EXPERIMENTAL RESULTS

In a previous paper, we reported experimental results on the dynamic fracture of a notched steel specimen (Rittel *et al.*, 1992). The apparent mode I fracture toughness was determined by measuring the time to fracture with a single-wire fracture gage. Following the above-mentioned procedure, the presence of a mode II component can now be ascertained and its extent quantified. In this experiment, the crack to ligament length ratio was $a/w = 0.52$ and the time to fracture was 57 μs (with time origin synchronized with the load pulse on face 1). The whole experiment was simulated by an FEM calculation and COD

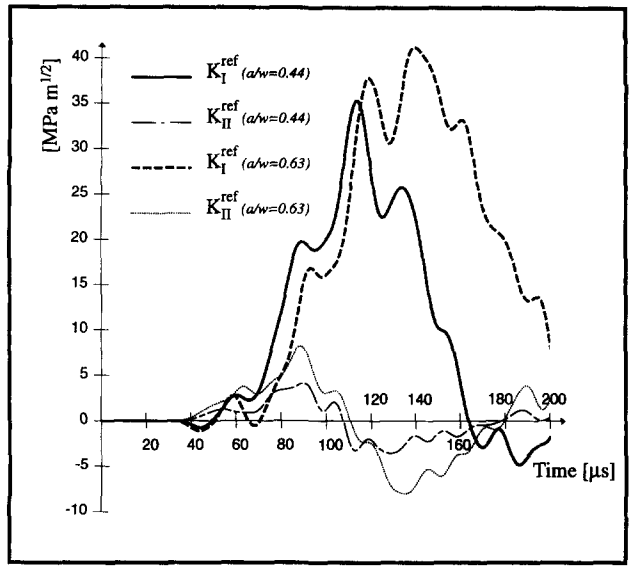

Fig. 4. PMMA reference specimen : calculated K_I and K_{II} stress intensity factors for $a/w = 0.44$ and $a/w = 0.63$.

values were extracted. Thus, similarly to the procedure adopted for mode I, the mode II component was determined by linear deconvolution (experimental data) and from the calculated COD values. Attention should be paid to the fact that for the mode I, we used the *symmetric* part of the recorded interfacial forces [$F_{I\exp}$ in eqn 4(a)]. For the mode II calculations, we used the *anti-symmetric* part [$F_{II\exp}$ in eqn (4b)] (Fig. 6). As shown in Fig. 7, a very good agreement is observed between experimental and calculated values of the mode II stress intensity factors. One remark can be made concerning the numerical model. A shift of about 10 μs is noticeable between the experimental and the calculated mode II results whereas mode I results are well synchronized. This problem may well arise from the fact that perfect specimen–bar interfaces were assumed (Bui *et al.*, 1992), with a greater influence on mode II calculations. The mode-mixity parameter is plotted in Fig. 8 and it can be seen that the mode II component has a negligible contribution by the time fracture occurs. The values reported here pertain to apparent stress intensity factors since the specimen contained a blunt notch rather than a sharp crack. These values are reported only

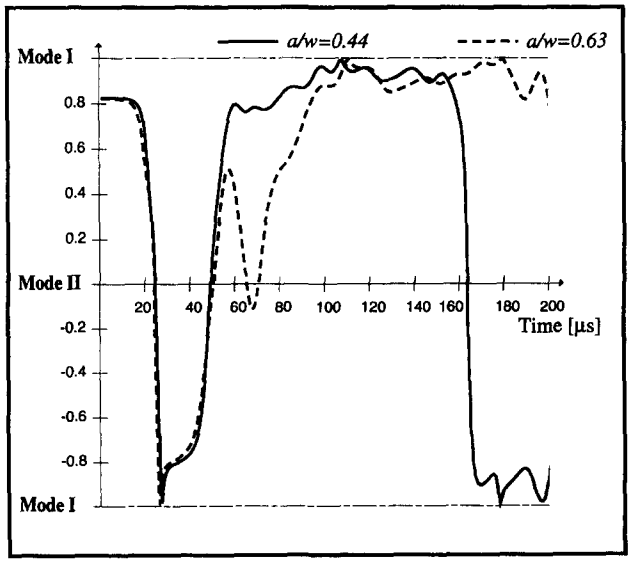

Fig. 5. PMMA reference specimen : mixity parameter for $a/w = 0.44$ and $a/w = 0.63$.

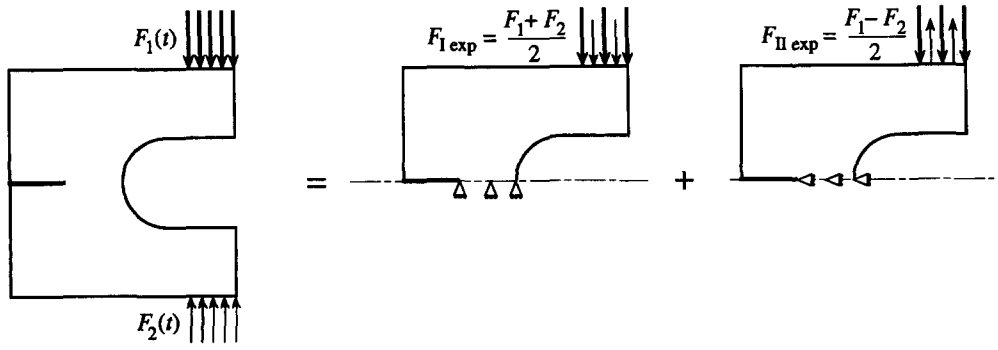

Fig. 6. Decomposition of an arbitrary loading, $F_1(t)$ and $F_2(t)$, into symmetric and anti-symmetric components used for mode I and mode II calculations.

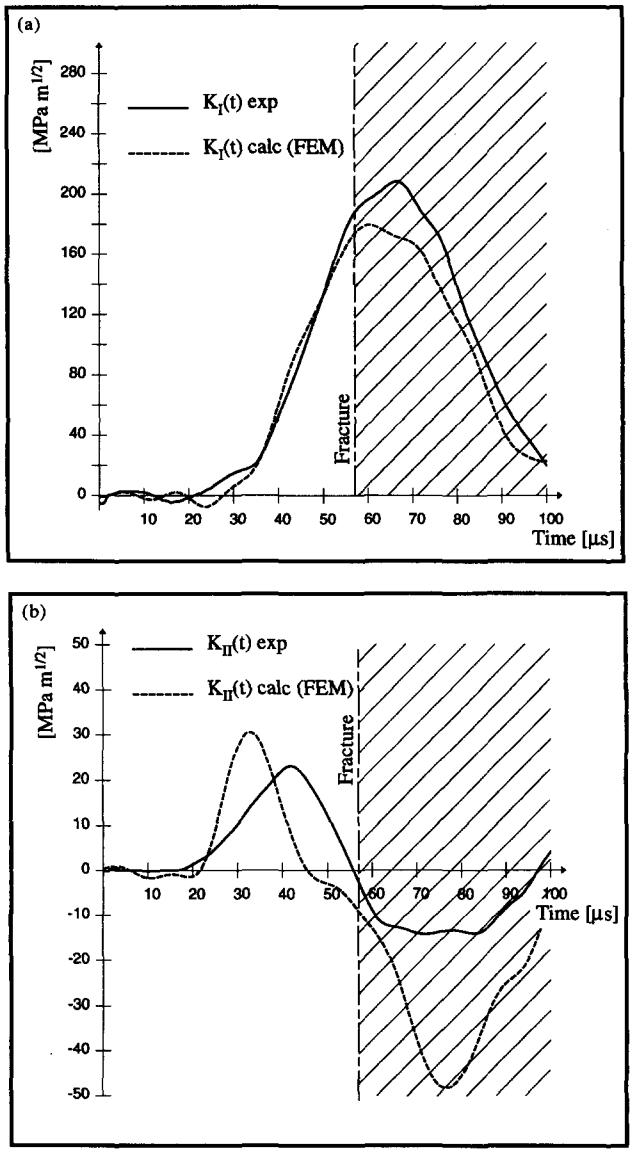

Fig. 7. Notched steel specimen ($a/w = 0.52$). Experimentally (linear deconvolution) and numerically (FEM) determined (a) mode I [reproduced from Rittel *et al.* (1992)] and (b) mode II stress intensity factors. Both curves have the same time origin. Results are not valid past fracture time (57 μs).

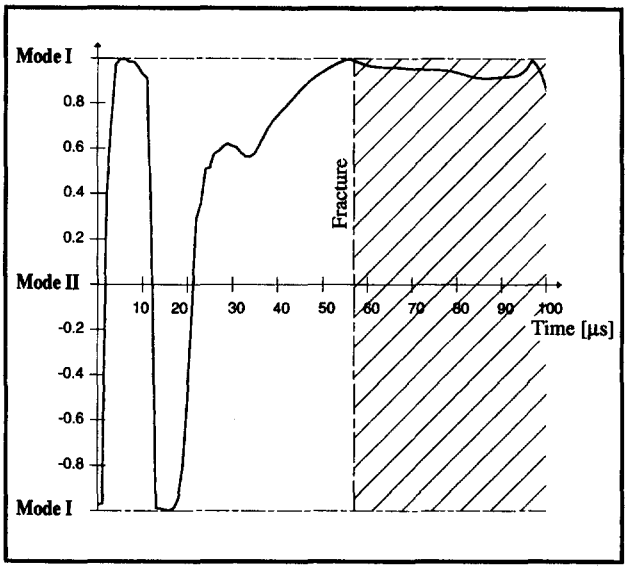

Fig. 8. Notched steel specimen: mixity parameter.

to provide an order of magnitude rather than a value of the dynamic fracture toughness of this material and the specimen (Rittel *et al.*, 1992).

Next, we report results for a fractured PMMA specimen, with properties listed in Table 1, notch to ligament length ratio of $a/w = 0.47$ and notch root radius smaller than 2.0×10^{-4} m. In this test, fracture was recorded after 108 μs. Testing was carried out in conditions identical to those used for the previous specimen except for the fact that a longer striker was used. This resulted in an incident pulse about 350 μs long. For this experiment, we used a single-wire commercial fracture gage (MM model CD 02 15A). Experimental recordings of the incident pulse (recorded on the incident bar) and the interfacial forces are shown in Fig. 9. It is worth noting that fracture occurred in a shorter time than that required for a complete transit of the (incident minus reflected) pulse through the specimen as it reaches the first (incident bar–CCS) interface (108 vs 350 μs). Consequently, the first interfacial force decreases markedly after 108 μs. Simultaneously, there is almost no discernible pulse recorded on the second (CCS–transmitter bar) interface until that time. This indicates that

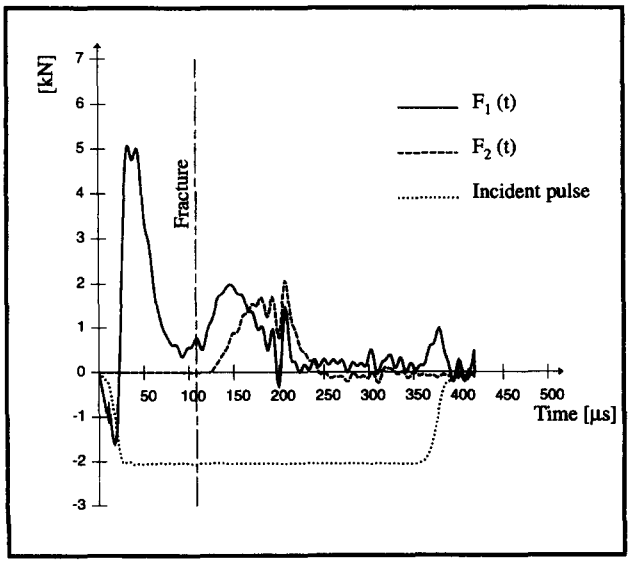

Fig. 9. Notched PMMA specimen ($a/w = 0.47$). Incident pulse (arbitrary units) and corresponding interfacial forces. Fracture occurred after 108 μs.

fracture occurred in a purely dynamic fashion due to the specimen's inertia (as it happens in one-point bending experiments). A different type of numerical simulation of the experiment was carried out. Rather than simulating the specimen-bars assembly, we used the finely meshed half CCS to which we applied F_{Iexp} once and F_{IIexp} once to isolate mode I and mode II respectively, in the spirit of Fig. 6. Figure 10 shows plots of the stress intensity factors determined once from the experimental and once from the numerically generated data. The two kinds of results are very similar until fracture and mode II is negligible by that time. It can also be noted that experimental and numerical mode I and mode II results are better synchronized, mostly for mode II calculations [compare Figs 7(b) and 10(b)]. This indicates that when the whole assembly is simulated, the assumption of perfect interfaces can cause a delay between numerical and experimental mode II results.

Furthermore, the present results also show that for this kind of dynamic fracture experiment, accurate determination of the time to fracture is very important since this parameter defines the crack initiation mode.

For this specimen, fracture toughness was found to be 3.79 MPa$\sqrt{\text{m}}$ at a loading rate of $\dot{K} = 1.15\text{E}05$ MPa$\sqrt{\text{m}}$ s^{-1} (defined as the dynamic fracture toughness divided by the

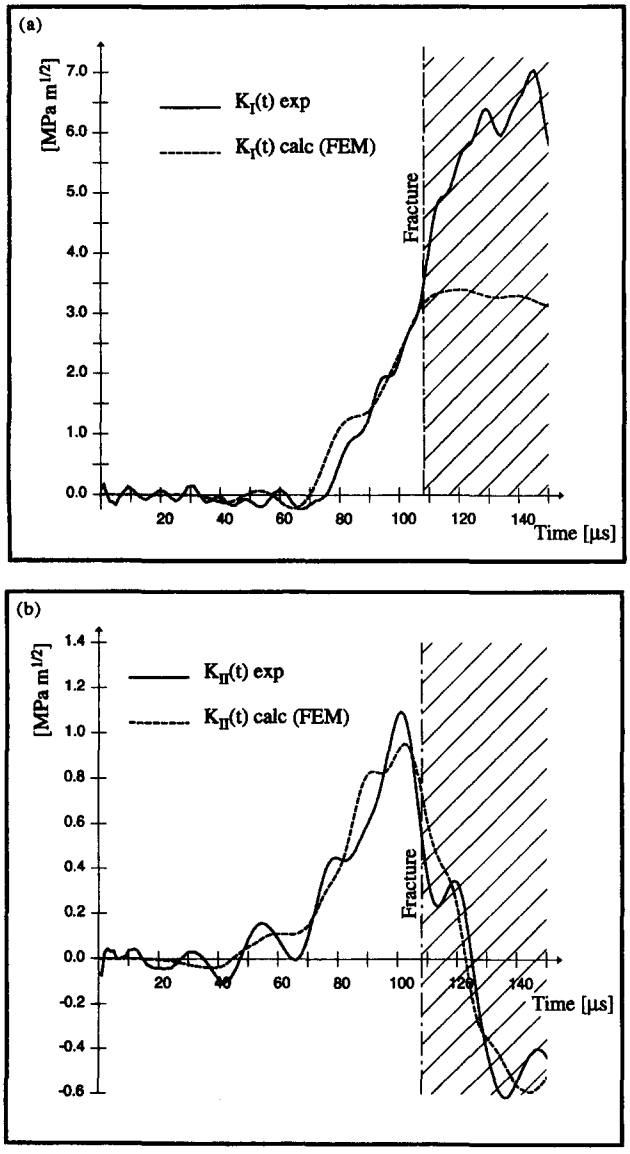

Fig. 10. Notched PMMA specimen. Experimentally (linear deconvolution) and numerically (FEM) determined (a) mode I, (b) mode II stress intensity factors and (c) mixity parameter. Results are not valid past fracture time (108 μs).

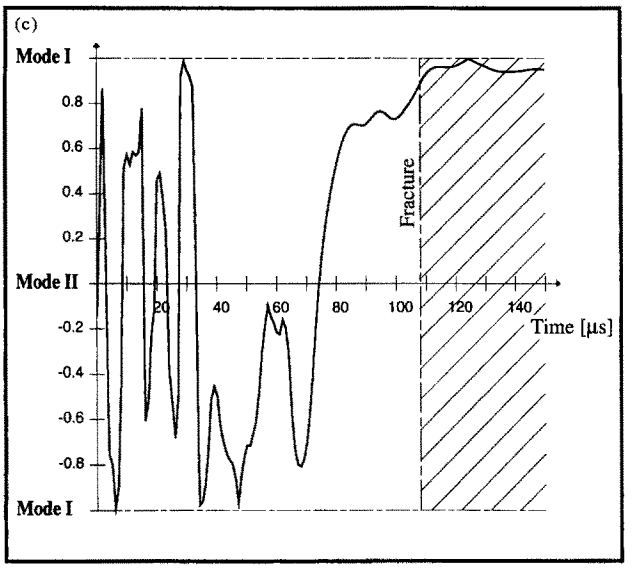

Fig. 10. *Continued.*

time to fracture). Here, the use of a notch rather than a sharp crack is not deemed to alter significantly the fracture toughness of this relatively brittle material. Indeed, our result agrees satisfactorily (at least to a first extent due to the limited sample size) with the results of Wada (1992) and Wada *et al.* (1992) who measured a value of 3.68 MPa$\sqrt{\text{m}}$ at $\dot{K} = 9.0\text{E}04$ MPa$\sqrt{\text{m}}$ s^{-1} using one point bend fracture tests of notched bars. Unfortunately, mode mixity was not addressed in this study though one can reasonably assume a dominant mode I since both the specimen geometry and the applied loads are symmetric.

It must be emphasized that numerical simulations of the experiment (using either the whole assembly or the half CCS with appropriate forces) are not required to determine the evolution of the stress intensity factors. Although they provide an excellent estimate of the interfacial velocities and stress intensity factors, the only purpose of these simulations is to enable a comparison between a simple numerical model and actual experimental results. By contrast, the main advantage of the present method is that a large volume of experimental results can be readily analysed using the linear deconvolution procedure without performing one FE calculation per specimen.

Finally, we have not attempted to "optimize" the shape or size of the CCS as mixed mode can neither be avoided simply nor can it be controlled beforehand. Rather, the present work is aimed at identifying and quantifying each mode component for a better analysis of experimental results.

5. CONCLUDING REMARKS

Mode-mixity develops in numerous dynamic fracture experiments and this phenomenon is difficult to avoid. Nevertheless, its extent can be quantified to provide a better estimation of experimental results about crack initiation.

The general expression for the H-integral under arbitrary loading has been decomposed into pure I and II modes. Path independence of the H-integral has been verified numerically both for mode I and mode II in the case of the CCS. This verifies by the same token consistency between boundary displacements and the corresponding stress intensity factors used as a set of references to determine the experimental stress intensity factor by linear deconvolution.

Mode I and II stress intensity factors have been determined numerically and compared for the reference CCS. It was observed that mode I rapidly becomes the predominant crack opening mode past a short period of mode-mixity. The same trend was also observed by

Kalthoff *et al.* (1992) for Izod-like specimens. Consequently, the crack initiation mode can be clearly defined provided accurate measurement of the time to fracture.

The degree of mode mixity was found to be relatively constant for two different crack to ligament length ratios (0.44 and 0.63).

Mixed mode components have been quantified for two sample experiments, one on a steel specimen and the other on a PMMA specimen. In both cases, mode I was observed to be the predominant crack initiation mode with a minor mode II contribution. Experimental results for the dynamic fracture toughness of PMMA are in good agreement with other published results using a different approach.

Acknowledgements—The authors would like to acknowledge useful discussions with H. D. Bui.

REFERENCES

Bui, H. D. (1983). Associated path independent J-integrals for separating mixed modes. *J. Mech. Phys. Solids* **31**(6), 439–448.

Bui, H. D. and Maigre, H. (1988). Fracteur d'intensité dynamique des contraintes tiré des grandeurs mécaniques globales. *C. R. Acad. Sc. Paris.* **t.306,** Série II, 1213–1216.

Bui, H. D., Maigre, H. and Rittel, D. (1992). A new approach to the experimental determination of the dynamic stress intensity factor. *Int. J. Solids Structures* **29**(23), 2881–2895.

Freund, L. B. (1990). *Dynamic Fracture Mechanics.* Cambridge University Press, Cambridge.

Freund, L. B. and Rice, J. R. (1974). On the determination of elastodynamic crack tip stress fields. *Int. J. Solids Structures* **10,** 411–417.

Gurtin, M. E. (1976). On a path-independent integral for elastodynamics. *Int. J. Fract.* **12,** 643–644.

Irwin, G. R. (1957). Analysis of stresses and strains near the end of a crack traversing a plate. *J. Appl. Mech.* **24**(3), 361–364.

Kalthoff, J. F. and Podleschny, R. (1992). On the nonsymmetry of the loading condition in Izod-type impact test configurations. In *Proceedings of the International Symposium on Impact Engineering* (Edited by I. Maekawa), pp. 605–610. Sendai.

Lee, Y. J. and Freund, L. B. (1990). Fracture initiation due to asymmetric impact loading of an edge cracked plate. *J. Appl. Mech.* **57,** 104–111.

Mason, J. J., Lambros, J. and Rosakis, A. J. (1992). The use of a coherent gradient sensor in dynamic mixed-mode fracture mechanics experiments. *J. Mech. Phys. Solids* **40**(3), 641–661.

Nakano, M., Kishida, K. and Watanabe, Y. (1992). Mixed-mode impact fracture tests using center-notched disk specimens. In *Proceedings of the International Symposium on Impact Engineering* (Edited by I. Maekawa), pp. 581–586. Sendai.

Nilsson, F. (1973). A path-independent integral for transient crack problems. *Int. J. Solids Structures* **9,** 1107–1115.

Rittel, D., Maigre, H. and Bui, H. D. (1992). A new method for dynamic fracture toughness testing. *Scripta Metall. et Mater.* **26,** 1593–1598.

Shih, C. F. (1974). Small-scale yielding analysis of mixed mode plane-strain crack problems. *Fracture Analysis.* ASTM STP 560, pp. 187–210.

Tippur, H. V., Krishnaswamy, S. and Rosakis, A. J. (1991). Optical mapping of crack tip deformations using the method of transmission and reflection coherent gradient sensing: a study of crack-tip K-dominance. *Int. J. Fract.* **52,** 91–117.

Wada, H. (1992). Determination of dynamic fracture toughness for PMMA. *Engng Fract. Mech.* **41**(6), 821–831.

Wada, H., Calder, C. A., Kennedy, T. C. and Seika, M. (1992). Measurement of impact fracture toughness with single point bending using air gun. In *Proceedings of the International Symposium on Impact Engineering* (Edited by I. Maekawa), pp. 569–574. Sendai.

Zhao, H. (1992). Analyse de l'essai aux barres de Hopkinson. Application à la mesure du comportement dynamique des matériaux. Doctoral Thesis. Ecole Nationale des Ponts et Chaussées, Paris.

APPENDIX

Following one reviewer's suggestion it seems desirable to clarify the relation between the H-integral, the concept of dynamic weight functions and other elastodynamic integrals. An expression for $K(t)$ which involves transient weight functions h and load p can be found, e.g. in Freund's eqn (5.7.1) (1990):

$$K_I(t) = \int_0^t \int_B h(x_B, t-\tau) p(x_B, \tau)\, dx_B\, d\tau. \tag{A1}$$

It can be shown that this expression can be related to the H-integral.

To this effect suppose that in eqn (2) the reference field $\mathbf{v}$ can be found such as $K_{id}^{v} \equiv \delta(t)$ (Dirac function). Using the property of convolution products eqn (2) writes now:

$$K_{id}^{u} * \delta = K_{id}^{u}(\tau) = H(\tau; \mathbf{u}, \mathbf{v}) \quad i = \mathrm{I}, \mathrm{II}. \tag{A2}$$

In this case the dynamic weight function can be identified from eqn (1a) as:

$$h \equiv \left(\frac{\partial \mathbf{v}}{\partial a}, \frac{\partial \mathbf{T}[\mathbf{v}]}{\partial a} \right). \tag{A3}$$

Next, as previously remarked (Bui *et al.*, 1992) it should be noted that the (actual) experimental field $\mathbf{u}$ is available for a *finite* time interval $[0, t_{exp}]$ only. The convolution products in eqns (1)–(3) are thus strictly defined for $\tau \in [0, t_{exp}]$. For practical applications, this precludes us from using Laplace transforms of the relevant fields which would thus need to be defined over an *infinite* time interval. In this respect, the derivation of the H-integral by the adjoint field theory differs slightly from other path-independent integrals.